

from Forbes leads to $\sigma_c = 0.06 \pm 0.09$ barn. σ_{is} becomes 1.0 ± 0.2 barns for the normal isotopic mixture.

Cadmium, Tin, Gold, Lead, and Bismuth

For these materials only permissible limits of the cross section are presented as shown in Table III.

Behavior of σ_i

The inelastic-collision cross sections reported here increase somewhat the precision with which a comparison may be made with the theory of nuclear interactions of Weisskopf and his associates.^{27,28} Figure 2 portrays the behavior of the quantity $[(\sigma_i/\sigma_c)-1]$ where the values of σ_i , the total cross section for 14.1-Mev neutrons are taken from Coon, Graves, and Barschall.²⁹ The \times points refer to values of σ_i reported here and the circles to values obtained by Phillips *et al.*¹⁵ Although the measurements on beryllium are not reported here, a preliminary value is included in the curve. A curve through the \times points and another through the circles are drawn to indicate a band which portrays the general behavior of the experimental quantity. The inelastic collision cross section σ_i experi-

mentally determined is identified with σ_c for compound nucleus formation from the theory where

$$\sigma_t = \sigma_c + \sigma_{sc}.$$

Hence $[(\sigma_i/\sigma_c)-1]$ is equivalent to (σ_{sc}/σ_c) from the theory. The curve marked "THEORY" shows (σ_{sc}/σ_c) upon the assumption that the nuclear radius = $1.5 \times 10^{-13} A^{1/3}$ cm. Although this theory is undergoing revision, it is felt that the comparison as shown is a useful one since it deals with a fairly fundamental concept. It also shows clearly the regions of atomic mass which need further investigation to better establish the empirical curve.†

‡ *Note added in proof.*—Further investigation of the region between carbon and iron has been made. Preliminary values of the inelastic collision cross section, σ_i , have been obtained for F, S, KCl, Ca, Sc, Ti, and V. These show a discontinuity in the curve of σ_i vs $A^{1/3}$ between Ca and Sc, preceded by a smooth rise of σ_i to 1.5 ± 0.1 barn for Ca. Beginning with Sc the values fall on a new smooth curve which extrapolated to lower masses would join the lower branch between F and Al. The preliminary value of σ_i for Ti is 1.23 ± 0.04 barns and for V is 1.32 ± 0.08 barns. These results in conjunction with total cross sections (see reference 29) give additional experimental points for $[(\sigma_i/\sigma_c)-1]$ as a function of $A^{1/3}$ as shown in Fig. 2. From $A^{1/3} = 3.00$ the points continue to drop through 0.58 ± 0.07 for $A^{1/3} = 3.3 \pm 0.1$ (KCl) to 0.43 ± 0.10 for $A^{1/3} = 3.42$ (Ca). For the next higher $A^{1/3}$ values, Sc and Ti, the values are on a rising curve. For $A^{1/3} = 3.63$ (Ti) the preliminary value is 0.85 ± 0.10 . Further measurements are in progress.

²⁷ H. Feshbach and V. F. Weisskopf, Phys. Rev. **76**, 1550 (1949).
²⁸ J. M. Blatt and V. F. Weisskopf, *Theoretical Nuclear Physics* (John Wiley and Sons, Inc., New York, 1952), Chap. VIII, Sec. 4.
²⁹ Coon, Graves, and Barschall, Phys. Rev. **88**, 562 (1952).

Alignment of Cerium-141 and Neodymium-147 Nuclei*†

E. AMBLER AND R. P. HUDSON, *National Bureau of Standards, Washington, D. C.*

AND

G. M. TEMMER, *Department of Terrestrial Magnetism, Carnegie Institution of Washington, Washington, D. C.*

(Received November 1, 1954)

The radioactive nuclei Ce^{141} and Nd^{147} have been aligned by the magnetic hfs method (Bleaney) using single crystals of cerium magnesium nitrate. The cerium site is characterized by $B \gg A$, i.e., the "alignment" occurs in a plane. The anisotropies for the 142-kev gamma ray of Ce^{141} , and the 92-kev and 530-kev gamma rays of Nd^{147} , at the lowest temperature (0.00308°K) were found to be +0.12, 0, and -0.39, respectively. These values coupled with the rate of change of anisotropy with temperature identify the transitions as $M1$, $M1+E2$, and $E2$, respectively. The decay schemes supported by these experiments are as follows: Ce^{141} (142 kev), $7/2^- \rightarrow 7/2^+ \rightarrow 5/2^+$; Nd^{147} (92 kev), $9/2^- \rightarrow 7/2^+ \rightarrow 5/2^+$; Nd^{147} (530 kev), $9/2^- \rightarrow 9/2^+ \rightarrow 5/2^+$. From the temperature dependence of the anisotropies we can deduce values for the magnetic moments as follows: Ce^{141} , 0.16 ± 0.06 nm; Nd^{147} , 0.22 ± 0.05 nm. These rather small values for odd-neutron nuclei may not be meaningful because of possible internal magnetic field effects in the crystal which are not taken into account in the treatment of the hyperfine interaction.

1. INTRODUCTION

TO date, two of the methods which have been proposed for producing oriented nuclear systems at low temperatures have been carried out successfully.

* Supported in part by the Office of Naval Research, under contract with the National Bureau of Standards.

† A preliminary account of the work on cerium-141 was given at the Spring Meeting of the American Physical Society, April 29–May 1, 1954 [Ambler, Hudson, and Temmer, Phys. Rev. **95**, 625 (1954)].

Both methods rely on the fact that at the nucleus of certain paramagnetic ions there exists a very large magnetic field (10^5 – 10^6 oersteds, produced by the unpaired electrons in the unfilled shell) which couples together the electron and nuclear magnetic moments, and produces a considerable hyperfine splitting.

In one method, suggested independently by Gorter¹

¹ C. J. Gorter, *Physica* **14**, 504 (1948).

and by Rose,² the proposal was to apply a fairly small magnetic field (100–1000 oersteds) to a suitable paramagnetic salt at a very low temperature, so that the electron moments would be polarized almost to saturation. The temperature, T , should be sufficiently low ($\sim 0.01^\circ\text{K}$) so that kT is of the order of the hyperfine splitting; under these circumstances only the lowest of the hyperfine levels would be populated, corresponding to a nuclear polarization along the direction of the magnetic field. This principle has been applied to polarize assemblies of the nuclei Co⁶⁰,³ Mn⁵⁵,⁴ and Sm¹⁴⁹.⁵

The other method, which was proposed by Bleaney,^{6,7} produces an *alignment* of the nuclei rather than a *polarization* and there is preferential orientation, both parallel and antiparallel to a certain direction in space; in other words, states with positive and negative values of the magnetic quantum number have the same energy. This, however, is of no consequence if the aim is to orient radioactive nuclei and to observe the polar diagram of the emission of gamma rays, since the pattern of the radiation is symmetrical with respect to a plane perpendicular to the axis of quantization of the nucleus.⁸ No external magnetic field is necessary in this method. It relies entirely on the fact that in certain paramagnetic salts, the crystalline electric field produces anisotropic hyperfine splitting, so that the energy of interaction between nuclear and electron magnetic moments depends not only upon their relative orientation, but also upon their orientation with respect to some preferred axis within the crystal. In other words, the magnitude of the magnetic field at the nucleus depends upon the direction of the electron moment relative to this axis.

The problem of nuclear orientation has been discussed by Bleaney in terms of the spin-Hamiltonian. In many paramagnetic crystals the hyperfine structure is symmetrical with respect to a particular axis, and if the axis is taken to be the z -axis, the magnetic interaction can be written

$$\mathcal{H}C = AS_zI_z + B(S_xI_x + S_yI_y),$$

where S_x , S_y , and S_z are the components of the electron spin operator, and I_x , I_y , and I_z the components of the nuclear spin operator. A and B are constants which can be determined from paramagnetic resonance experiments. When the lowest electronic level is a doublet, S is set equal to $1/2$ and the two extreme cases (i) $A \gg B$, and (ii) $B \gg A$, are favorable for producing alignment.

(i) When $A \gg B$, the levels consist of a set of $(2I+1)$

² M. E. Rose, Phys. Rev. **75**, 213 (1949).

³ Ambler, Grace, Halban, Kurti, Durand, Johnson, and Lemmer, Phil. Mag. **44**, 216 (1953).

⁴ Bernstein, Roberts, Stanford, Dabbs, and Stevenson, Phys. Rev. **94**, 1243 (1954).

⁵ Roberts, Bernstein, Dabbs, and Stanford, Phys. Rev. **95**, 105 (1954).

⁶ B. Bleaney, Proc. Phys. Soc. (London) **A64**, 315 (1951).

⁷ B. Bleaney, Phil. Mag. **42**, 441 (1951).

⁸ J. A. Spiers, Nature **161**, 807 (1948).

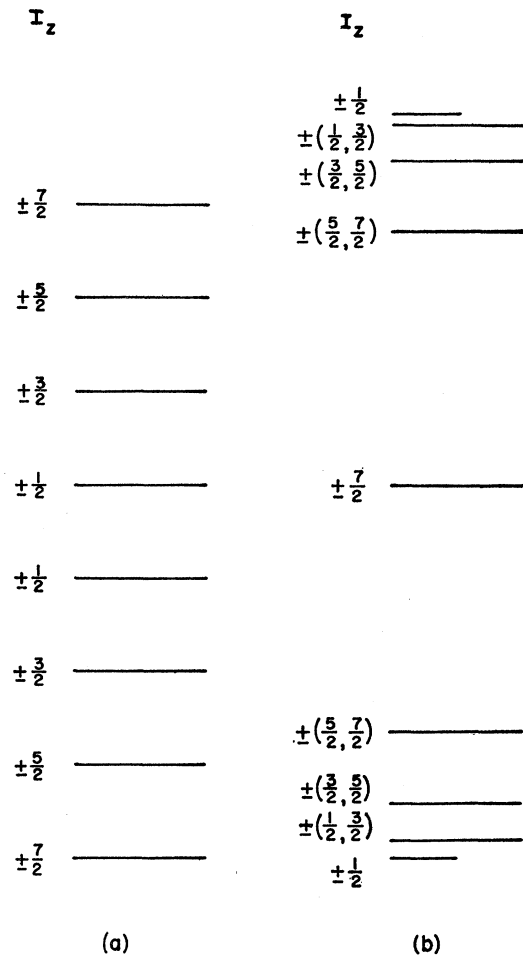


FIG. 1. Hyperfine energy levels for the case of nuclear spin $I=7/2$. (a) $A \gg B$, favorable for axial alignment; (b) $B \gg A$, favorable for "alignment" in a plane. A and B are hyperfine splitting constants in the spin-Hamiltonian.

doublets spaced by an energy interval $A/2$; the lowest level is characterized by $I_z = \pm I$, the next by $I_z = \pm(I-1)$ and so on, as shown in Fig. 1(a) for the particular case $I=7/2$. At a sufficiently low temperature, therefore, the nuclear spins will become aligned along the direction of the z -axis. This method has been used for aligning various radioactive cobalt nuclei.⁹⁻¹⁷

⁹ Daniels, Grace, and Robinson, Nature **168**, 780 (1951).

¹⁰ Gorter, Poppema, Steenland, and Beun, Physica **17**, 1050 (1951).

¹¹ Bleaney, Daniels, Grace, Halban, Kurti, and Robinson, Phys. Rev. **85**, 688 (1952).

¹² Bleaney, Daniels, Grace, Halban, Kurti, Robinson, and Simon, Proc. Roy. Soc. **A221**, 170 (1954).

¹³ Poppema, Beun, Steenland, and Gorter, Physica **18**, 1235 (1952).

¹⁴ Gorter, Tolhoek, Poppema, Steenland, and Beun, Physica **18**, 135 (1952).

¹⁵ Bishop, Daniels, Goldschmidt, Halban, Kurti, and Robinson, Phys. Rev. **88**, 1432 (1952).

¹⁶ Daniels, Grace, Halban, Kurti, and Robinson, Phil. Mag. **43**, 1297 (1952).

¹⁷ M. A. Grace and H. Halban, Physica **18**, 1227 (1952).

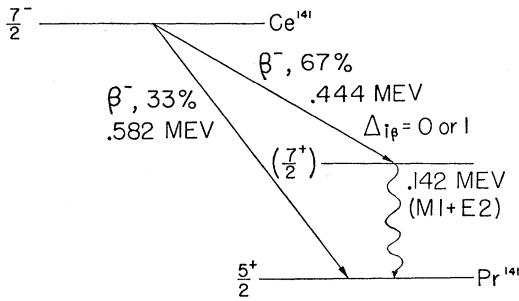


FIG. 2. Decay scheme of Ce^{141} , according to Kondaiah (see reference 18).

(ii) When $B \gg A$, the energy levels are as shown in Fig. 1(b), again drawn for $I=7/2$; in this case it is necessary to go to a much lower temperature to produce a high degree of alignment, partly on account of the crowding together of the lower energy levels, and partly because the lowest level has only half the degeneracy of the others. The lowest and highest levels are characterized by $I_z = \pm 1/2$, and the others, apart from the $I_z = \pm 7/2$ level, contain equal amounts of two adjacent nuclear magnetic substates, as shown in Fig. 1(b). At a low enough temperature the nuclei will precess about the z -axis in the $I_z = \pm 1/2$ state and we have, effectively, "alignment" in a plane perpendicular to the z -axis. It is this type of alignment which occurred in the experiments on Ce^{141} and Nd^{147} to be described.

2. NUCLEAR PROPERTIES

(a) Ce^{141}

The decay scheme of 30-day Ce^{141} as given, for example, by Kondaiah,¹⁸ is shown in Fig. 2. The beta ray to the excited state of Pr^{141} has an upper energy limit of 0.444 Mev, the one to the ground state of Pr^{141} has an upper energy limit of 0.582 Mev. The gamma ray connecting these two states, which is the one observed in the experiments, has an energy of 142 keV and occurs in 67 percent of the disintegrations. The experimental values of the internal conversion coefficient and K to L conversion ratio¹⁹ are given in Table I, together with the predicted values^{20,21} for electric dipole ($E1$), electric quadrupole ($E2$), and magnetic dipole

TABLE I. Comparison of experimental and theoretical internal conversion coefficients for the 142-keV gamma ray of Ce^{141} (see references 19, 20, and 21).

Experimental	K-shell internal conversion coefficients			Experimental	K/L ratio		
	$E1$	$E2$	$M1$		$E1$	$E2$	$M1$
0.48	0.08	0.42	0.43	6.5	9.5	4.6	6.3

¹⁸ E. Kondaiah, Arkiv Fysik 4, 81 (1951).

¹⁹ S. Johansson, Arkiv Fysik 3, 533 (1952).

²⁰ Rose, Goertzel, Harr, Spinrad, and Strong, Phys. Rev. 76, 184 (1949).

²¹ M. Goldhaber and A. W. Sunyar, Phys. Rev. 83, 906 (1951).

($M1$) radiation. Internal conversion data do not permit distinction between $M1$ and $E2$ radiation, although they certainly eliminate $E1$; the K to L ratio favors $M1$ over $E2$ though not as decisively as Table I would indicate, since the experimental value is uncertain by about 20 percent. As we shall explain later, it is just this sort of problem that can often be settled rather easily by the method of nuclear alignment. The ground-state spin of Pr^{141} is known to be $5/2$ and is classified as a $d_{5/2}$ state by the shell model, i.e., its parity is even. The $\log ft$ value of the ground-state beta transition is 7.75 and that for the excited-state transition is 7.00.¹⁸ According to Nordheim,²² both of these transitions can be classified as first-forbidden with a parity change, and spin change $\Delta i_\beta = 0$ or 1 (angular momentum carried away by the electron-neutrino field). Hence Ce^{141} should have odd parity and spin $3/2$, $5/2$, or $7/2$. According to the spin-orbit coupling scheme, the 83rd neutron outside the closed 82-neutron shell should be in an $h_{9/2}$ orbit, but an $f_{7/2}$ configuration occurs in the same shell and is not unlikely.

We shall therefore assume a spin of $7/2$ for Ce^{141} .

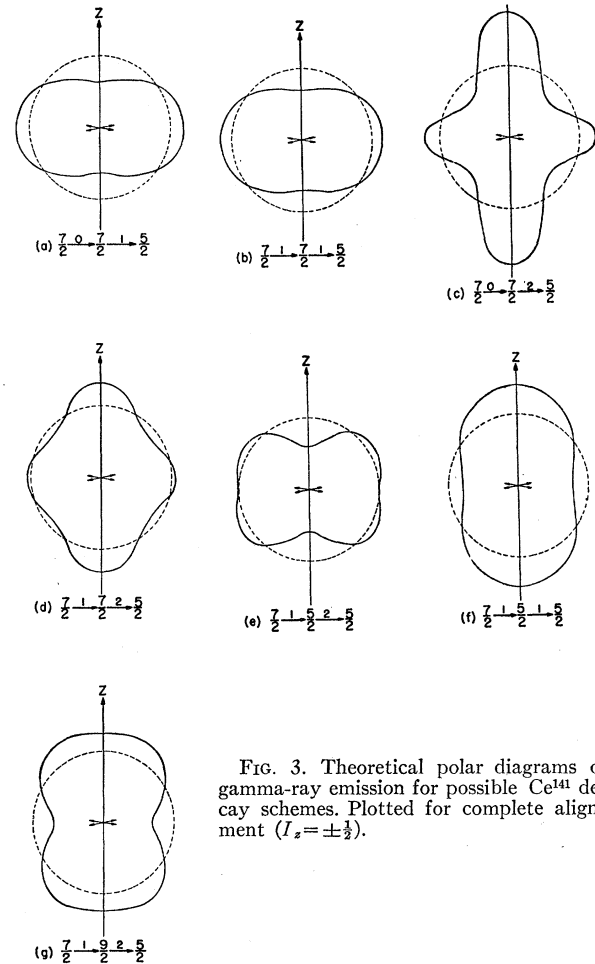


FIG. 3. Theoretical polar diagrams of gamma-ray emission for possible Ce^{141} decay schemes. Plotted for complete alignment ($I_z = \pm 7/2$).

²² L. W. Nordheim, Revs. Modern Phys. 23, 322 (1951).

The 142-keV level of Pr¹⁴¹ has even parity because of the *M1* or *E2* character of the gamma radiation. The first-forbidden beta decay allows its spin to be 5/2⁺, 7/2⁺, or 9/2⁺, unless the gamma radiation is at least partly *M1* in which case 9/2⁺ is ruled out.

From what has been said above, the following decay schemes are possible:

$$7/2 \xrightarrow{-1} 5/2 \xrightarrow{-1,2} 5/2; \quad 7/2 \xrightarrow{-0,1} 7/2 \xrightarrow{-1,2} 5/2; \\ 7/2 \xrightarrow{-1} 9/2 \xrightarrow{-2} 5/2.$$

In Fig. 3, we have plotted the corresponding polar diagrams to be expected for complete alignment in a plane (i.e., at $T=0$), using formulas given by Steenberg.²³ As an example we quote the expression for the angular distribution of gamma radiation for the decay scheme $7/2 \xrightarrow{-0} 7/2 \xrightarrow{-1} 5/2$ at $T=0$:

$$I(\theta) = 1 - (5/14)P_2(\cos\theta).$$

We thought it worth while, therefore, to carry out an experiment on the alignment of Ce¹⁴¹, with the primary objective of establishing the type of gamma transition involved.

(b) Nd¹⁴⁷

The decay scheme of 11-day Nd¹⁴⁷ has been studied by a number of authors.^{18,24,25} The gamma spectrum is believed to be rather complex²⁵ but there are only two gamma rays intense enough to be of interest in an

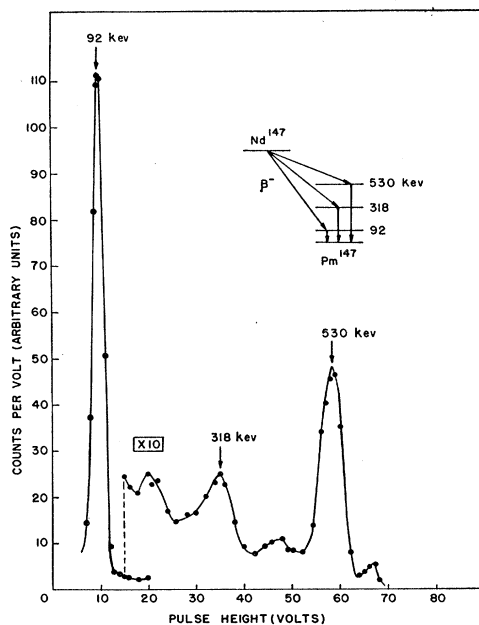


FIG. 4. Gamma-ray spectrum of Nd¹⁴⁷ obtained with 1 $\frac{1}{2}$ in. \times 2 in. NaI(Tl) scintillation crystal. Insert shows main portion of decay scheme.

²³ N. R. Steenberg, Proc. Phys. Soc. (London) **A65**, 791 (1952).

²⁴ W. S. Emmerich and J. D. Kurbatov, Phys. Rev. **83**, 40 (1951).

²⁵ Rutledge, Cork, and Burson, Phys. Rev. **86**, 775 (1952).

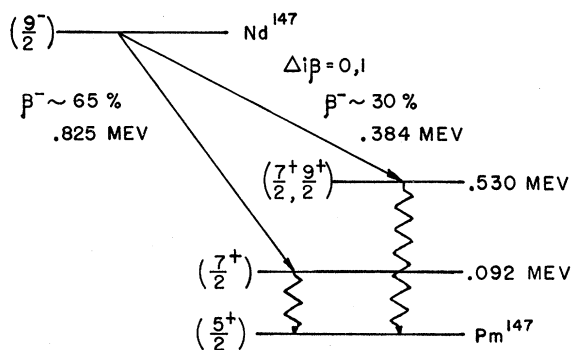


FIG. 5. Portion of decay scheme of Nd¹⁴⁷ of interest in this experiment.

alignment experiment, having energies 92 keV and 530 keV. Our scintillation spectrum of the gamma radiation emitted from our sample of Nd¹⁴⁷²⁶ is shown in Fig. 4. The 92-keV gamma ray is most intense and is known to be in coincidence with the most energetic beta-ray branch²⁴; it undoubtedly represents a ground-state transition. A comparison of its *K/L* conversion ratio (~ 7)^{18,27,28} with empirical curves of this ratio²¹ indicates either an *M1* transition, or an *M1+E2* transition, the *M1* component being predominant. The 530-keV gamma ray is known to be in coincidence with the 384-keV beta component; its *K/L* conversion ratio (5.7) points to an *E2* transition.²⁵

Figure 5 summarizes the portion of the decay scheme which is of interest here. The ground state of Pm¹⁴⁷ probably has spin 5/2⁺ ($d_{5/2}$ configuration); this is in keeping with the character of the first-forbidden beta transition ($\Delta i_{\beta}=1$) from this state to the ground state of Sm¹⁴⁷ whose spin has been measured to be 7/2.²⁹ The beta transitions to both the 92-keV and 530-keV levels in Pm¹⁴⁷ have $\log ft$ values indicating first-forbidden character with spin change 0 or 1 and a change in parity. Since these two levels are connected to the ground state by *M1* or *E2* transitions, their parities must be even, and Nd¹⁴⁷ must have odd parity. Nd¹⁴⁷ with 60 protons and 87 neutrons, is expected to have a $h_{9/2}$ configuration. This is corroborated by the fact that no direct beta ray to the ground state is observed, indicating a higher order of forbiddenness. Assuming this, we would predict:

(i) spin 7/2 for the 92-keV state in order to allow both a first-forbidden beta transition and *M1* gamma transition,

(ii) spin 7/2 or 9/2 for the 530-keV state in order to allow both a first-forbidden beta transition and either an *M1* or *E2* gamma transition. The possible decay schemes would then be: $9/2 \xrightarrow{-0,1} 9/2 \xrightarrow{-2} 5/2$; $9/2 \xrightarrow{-1} 7/2 \xrightarrow{-2} 5/2$; $9/2 \xrightarrow{-1} 7/2 \xrightarrow{-1} 5/2$. The

²⁶ Both Ce¹⁴¹ and Nd¹⁴⁷ were obtained from the Oak Ridge National Laboratory, Oak Ridge, Tennessee.

²⁷ J. W. Mihelich and E. L. Church, Phys. Rev. **85**, 690 (1952).

²⁸ A. B. Smith and A. C. G. Mitchell, Phys. Rev. **87**, 1128 (1952).

²⁹ K. Murakawa, Phys. Rev. **93**, 1232 (1954).

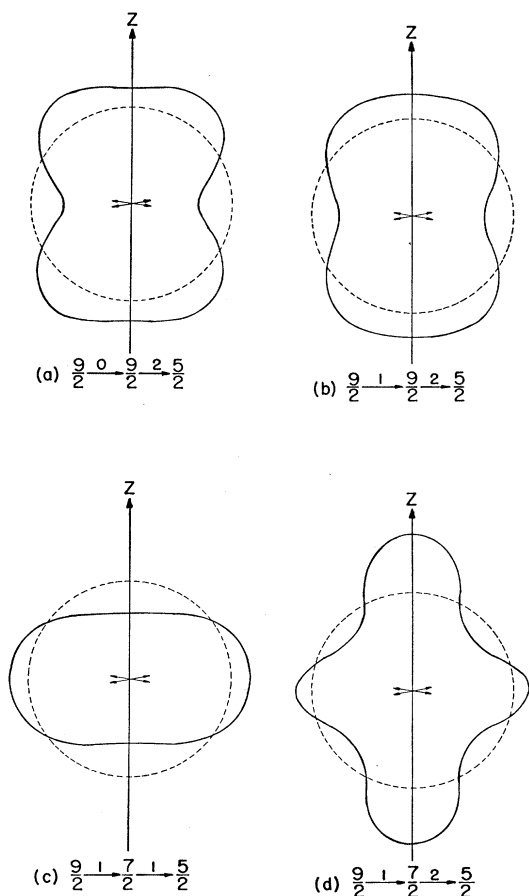


FIG. 6. Theoretical polar diagrams of gamma-ray emission for possible Nd^{147} (530 keV) decay schemes. Plotted for complete alignment ($I_z = \pm \frac{1}{2}$).

theoretical polar diagrams of emission of the gamma rays in these cases are shown in Fig. 6, for alignment in a plane at $T=0$. The angular distribution for the most likely case $9/2 \rightarrow 0 \rightarrow 9/2 \rightarrow 2 \rightarrow 5/2$ is given by:

$$I(\theta) = 1 + (10/21)P_2(\cos\theta) - (2/7)P_4(\cos\theta).$$

3. SOLID STATE PROPERTIES

(a) Cerium

In searching for a paramagnetic salt suitable for a nuclear alignment experiment it is usual to examine hyperfine splitting as determined by paramagnetic resonance experiments. Unfortunately, the naturally occurring isotopes of cerium are all even-even nuclei, hence have zero spin, and the paramagnetic resonance spectrum of the element shows no hyperfine structure. We are therefore entirely dependent upon theoretical predictions for the values of A and B . The theory of the Ce^{+++} ion has been given by Elliott and Stevens³⁰ with special reference to the salt cerium ethyl sulfate.

³⁰ R. J. Elliott and K. W. H. Stevens, Proc. Roy. Soc. (London) **A215**, 437 (1952).

This salt is not particularly useful for adiabatic demagnetization work, but cerium magnesium nitrate, to which one thought the theory would also apply, is in many respects an ideal substance. Daniels and Robinson³¹ investigated the thermal and magnetic properties below 1°K and showed that it is possible, by demagnetizing from 1°K and 14 kilo-oersteds, to reach a temperature of 0.00308°K. Here the salt has an appreciable specific heat so that it is possible to maintain this temperature for a usefully long period of time. Alignment would then depend upon the hyperfine splitting being of the order of 0.003°K, and markedly anisotropic.

The results of paramagnetic resonance experiments³² show that in the liquid-helium range of temperature the magnetic properties of the Ce^{+++} ion in cerium magnesium nitrate can be described by an effective spin $S=1/2$, with an anisotropic g -factor: $g_{\parallel}=0.25$ (along the z -axis) and $g_{\perp}=1.84$. It is possible to combine these results with theory to obtain the matrix elements needed in computing the values of A and B through the formulas³³:

$$A = \frac{4\beta\beta_n\mu_n}{I} \left\langle \frac{1}{r^3} \right\rangle_{Av} \left\langle +\frac{1}{2} | N_z | +\frac{1}{2} \right\rangle, \quad (1)$$

$$B = \frac{4\beta\beta_n\mu_n}{I} \left\langle \frac{1}{r^3} \right\rangle_{Av} \left\langle +\frac{1}{2} | N_x | -\frac{1}{2} \right\rangle, \quad (2)$$

where β is the Bohr magneton, β_n the nuclear magneton, μ_n the nuclear magnetic moment in nuclear magnetons, r the radial distance of the $4f$ electron from the nucleus, and \mathbf{N} a vector,

$$\mathbf{N} = \left\{ \mathbf{1} - \mathbf{s} + \frac{3(\mathbf{r} \cdot \mathbf{s})\mathbf{r}}{r^2} \right\},$$

which appears in the hyperfine interaction Hamiltonian,

$$\mathcal{H}_n = \frac{2\beta\beta_n\mu_n}{I} \left\langle \frac{1}{r^3} \right\rangle_{Av} \mathbf{N} \cdot \mathbf{I}.$$

We can see that the ratio of A to B is determined solely by the ratio of two matrix elements.

More recent calculations of Judd and Pryce³⁴ have shown that better agreement between theory and experiment is obtained if one assumes a slightly different symmetry for the crystalline electric field from that assumed by Elliott and Stevens. Their preliminary numerical values for the matrix elements in Eqs. (1) and (2) are 0.10 and 1.62, respectively. Thus if radioactive cerium nuclei possessing a magnetic moment are

³¹ J. M. Daniels and F. N. H. Robinson, Phil. Mag. **44**, 630 (1953).

³² Cooke, Duffus, and Wolf, Phil. Mag. **44**, 623 (1953).

³³ R. J. Elliott and K. W. H. Stevens, Proc. Roy. Soc. (London) **A218**, 553 (1953).

³⁴ B. R. Judd (private communication).

included in the double nitrate salt they will approximate closely to the case of $B \gg A$, and at a sufficiently low temperature there will result alignment in a plane.

(b) Neodymium

Hyperfine splittings have been observed in paramagnetic resonance spectra of the Nd^{+++} ion in neodymium magnesium nitrate³⁵ for the stable isotopes of mass numbers 143 and 145. The experiments show that at liquid helium temperatures the magnetic behavior can be described by a spin-Hamiltonian with $S=1/2$, $g_{||}=0.45$, and $g_{\perp}=2.73$. The hyperfine splitting constants are:

$$A_{143}=0.005 \text{ cm}^{-1}, \quad B_{143}=0.0312 \text{ cm}^{-1};$$

$$A_{145}=0.003_3 \text{ cm}^{-1}, \quad B_{145}=0.0194 \text{ cm}^{-1}.$$

Once again, therefore, we have the case of $B \gg A$, with alignment in a plane at sufficiently low temperatures. The ratio of the constants A and B for the radioactive isotope 147 to the corresponding constants for the stable isotopes will, of course, just equal the ratio of the respective nuclear gyromagnetic ratios.

4. EXPERIMENTAL METHOD

Cerium magnesium nitrate crystallizes in flat hexagonal plates with a width-to-thickness ratio of about 8:1; the axis perpendicular to the plate is the axis of low susceptibility, i.e., the z -axis. For each of the experiments, three such crystals were grown weighing altogether about 5 g and containing, at the beginning of the experiments, about 60 microcuries of activity. In the second series of experiments the neodymium re-

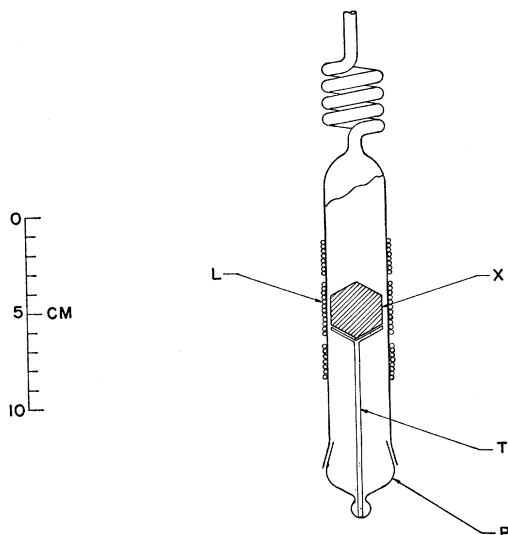


FIG. 7. Schematic diagram of demagnetization cryostat. X , radioactive crystal specimen; T , thin glass support; P , ground glass plug; L , mutual inductance secondary coil for susceptibility measurements.

³⁵ A. H. Cooke and H. J. Duffus, Proc. Roy. Soc. (London) (to be published).

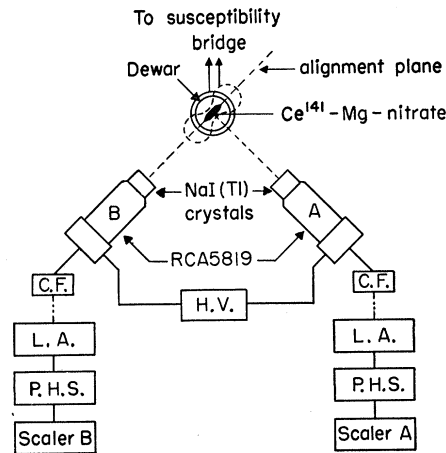


FIG. 8. Block diagram of counter array (plan view). A and B are scintillation counters; C.F., cathode followers; L.A., linear amplifiers; P.H.S., single-channel pulse-height selectors.

placed a very small fraction of cerium in the crystals. The latter, X , were mounted with the direction of their z -axes coincident and horizontal, inside a glass demagnetization cryostat as shown in Fig. 7. The support is a glass tube, T , 1.5 mm diameter and 0.2 mm wall thickness, which is attached to the ground-glass plug P . A vacuum-tight seal is made at the ground joint by means of a mixture described elsewhere.³⁶ The general arrangement of the pickup coils and ac bridge for measuring the susceptibility have also been described.³⁷ The whole cryostat was immersed in a Dewar of liquid helium jacketed by liquid nitrogen.

The salt was magnetized in a field of about 22 kilo-oersteds at 1.1°K along a direction of large magnetic susceptibility, i.e., along a direction in the plane of the crystals. This corresponded to an entropy given by $S/R=0.22$, and, as can be deduced from the table of results given in reference 31, this is well within the region of the large specific heat of the salt. After adiabatic demagnetization the apparatus was swung from the magnet into the counter array shown schematically in Fig. 8.

Two scintillation counter systems A and B were used, each consisting of a 1 in. \times 1 in. cylindrical sodium iodide crystal mounted on a RCA 5819 photomultiplier tube, followed by a conventional sequence of cathode follower, linear amplifier, single-channel pulse-height selector, and a scaling unit. A window of 2 volts was used which was sufficient to discriminate against a small amount of impurity radiation present, as well as wide-angle scattered (and hence energy-degraded) radiation. The latter point was checked by verifying the inverse-square dependence of counting rate upon distance. Counts were collected in both channels A and B over ten-second or twenty-second intervals starting about 30 seconds after de-

³⁶ R. P. Hudson and C. K. McLane, Rev. Sci. Instr. 25, 190 (1954).

³⁷ D. de Klerk and R. P. Hudson, J. Research Natl. Bur. Standards 53, 173 (1954).

magnetization, there being about ten seconds recording time between these intervals. Some 10 000 counts were recorded in each counter during each 10-second period for the 142-keV gamma ray in the Ce^{141} experiment. The counters were at a distance of 35 cm from the sample. Some 1000 and 5000 counts were recorded during each 20-second period for the 530-keV and 92-keV gamma rays, respectively, in the neodymium experiment. Because of lower gamma-ray intensities the counters were moved in to a distance 15 cm from the sample. Finite solid angle corrections to the anisotropy never exceeded 3 percent of the observed value (small compared to the statistical errors) and were not applied.

During each run the magnetic susceptibility of the specimen was monitored in order to determine its temperature. When too high an ac measuring field was used, we found that significant heating was produced in the specimen which rapidly warmed it to the helium bath temperature. Upon reducing this field to 0.1 oersted, the ac heating became negligible compared to that due to other sources, estimated to be about 100 erg/min. About half of this is accounted for by the heating due to radioactivity. The warmup time, during which there was a detectable anisotropy, was about eight minutes from the time of demagnetization.

5. RESULTS

(a) Ce^{141}

The results of a typical run are shown in Fig. 9, where we have plotted, as functions of time, the

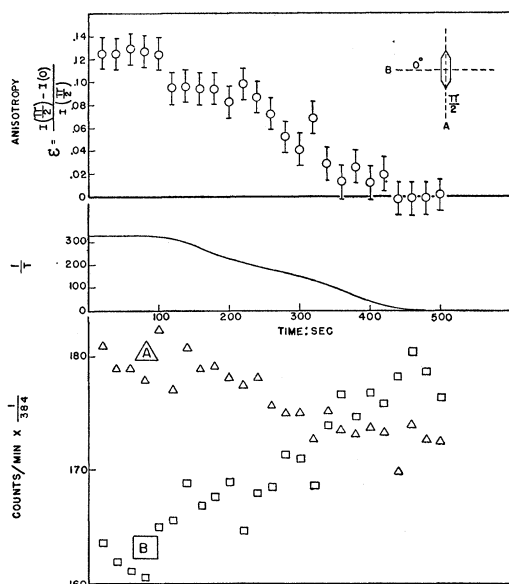


FIG. 9. Results of a single demagnetization in Ce^{141} experiment. Plotted against time are anisotropy (top), reciprocal of absolute temperature (center), and individual counting rates (unnormalized) of counters A (Δ) and B (\square). Each point represents a ten-second counting interval. Insert shows counter positions with respect to crystal axes.

individual counting rates of counters A and B , with B situated along the z -axis of the crystal and A perpendicular to it; $1/T$, the reciprocal of the absolute temperature; and the anisotropy $\epsilon = [I(\frac{1}{2}\pi) - I(0)]/I(\frac{1}{2}\pi)$, where $I(\theta)$ is the intensity measured in a direction making an angle θ with the z -axis of the crystal. It will be seen that, as the temperature increases, counting rate A decreases while B increases, and that ϵ is positive. The scatter of the points of the individual counting rates is mainly due to inaccuracies in timing the ten-second counting interval, a factor which does not affect the value of ϵ ; the limits shown for the values of ϵ are due to counting statistics only.

The average value of ϵ for a number of runs is plotted against $1/T$ in Fig. 10. Counters A and B were interchanged for about half of the runs and no difference could be noted in the results. The point at the lowest temperature ($T=0.00308^\circ\text{K}$, $\epsilon=0.12$) has a much smaller standard deviation than the others. This is because the salt remained at the lowest temperature

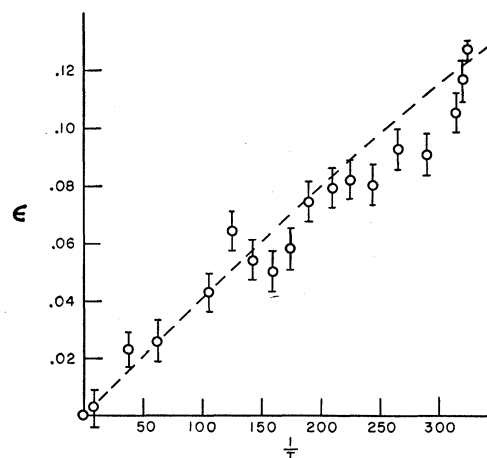


FIG. 10. Anisotropy (ϵ) vs reciprocal of absolute temperature ($1/T$) for Ce^{141} experiment. Points represent averages of ten demagnetizations. Note smaller statistical error at lowest temperature (see text).

for about 100 seconds during each of ten demagnetizations, allowing a greater number of counting periods than at any other temperature. Another reason why this point is most reliable is that the value of the absolute temperature is more accurately known. Since with cerium magnesium nitrate the absolute temperature remains substantially constant at 0.00308°K ³¹ over the wide entropy range $S/R=0.100$ to 0.425 , the absolute temperature of our specimen immediately after demagnetization ($S/R \approx 0.22$) is well known. However, when the temperature of the specimen rises above 0.00308°K due to unavoidable heat leaks, it must be determined from susceptibility measurements through the familiar $T^* \rightarrow T^\otimes \rightarrow T$ correlations.^{31,33} Because of the very small thermal conductivity of paramagnetic

³³ N. Kurti and F. E. Simon, *Phil. Mag.* **26**, 849 (1938).

salts at very low temperatures, extraneous heat leaks cause inhomogeneous heating of the specimen and any measured susceptibility represents an average value. Consequently the value of T^* obtained is an average value. In addition to this, it should be remembered that the conversion of T^* to T^\otimes is strictly permissible only in the case of an ellipsoidal specimen.³⁸

The general symmetry of the polar diagram of emission was verified by placing both counters in the alignment plane and perpendicular to each other (no anisotropy was observed) and also by placing both counters at 45° to the z -axis (again no anisotropy was detected).

(b) Nd^{147}

The results of a typical run are shown in Fig. 11 where we have plotted for the 530-keV gamma ray similar quantities to those shown in Fig. 8 for the gamma ray from Ce^{141} . It will be seen that in this case, as the temperature increases, counting rate A increases while B decreases (B again being on the z -axis) and that the relative changes in the counting rates are very nearly equal. The average value of the anisotropy ϵ for a number of runs is plotted against $1/T$ in Fig. 12; at the lowest temperature, $T=0.00308^\circ K$, $\epsilon=-0.39$. Measurements were also made with counter A at

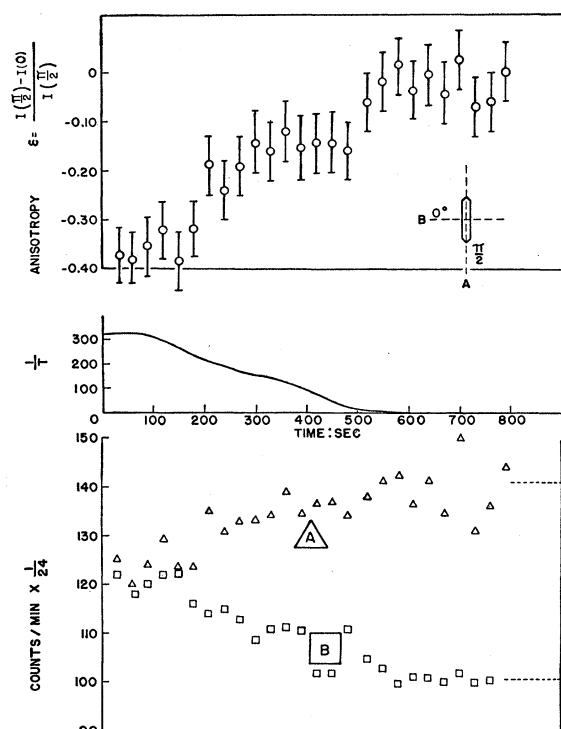


FIG. 11. Results of a single demagnetization in Nd^{147} experiment (530-keV gamma ray). Plotted against time are anisotropy (top), reciprocal of absolute temperature (center), and individual counting rates (unnormalized) of counter A (Δ) and B (\square). Each point represents a twenty-second counting interval. Insert shows counter positions with respect to crystal axis. Dotted horizontal lines indicate "warm" (isotropic) counting rates.

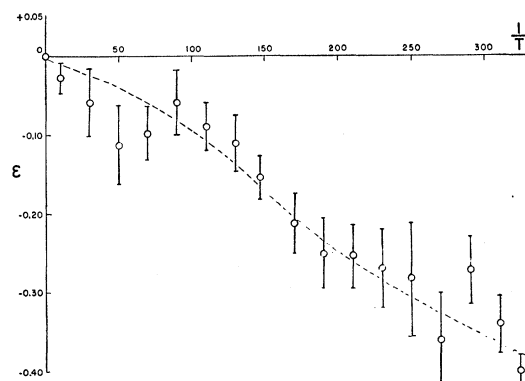


FIG. 12. Anisotropy (ϵ) vs reciprocal of absolute temperature ($1/T$) for Nd^{147} experiment (530-keV gamma ray). Points represent averages of fifteen demagnetizations. Note smaller statistical error at lowest temperature.

$\theta=50^\circ$, counter B remaining along the z -axis of the crystal. An anisotropy of 0.16 was observed.

No anisotropy greater than 0.05 was detected in the angular distribution of the 92-keV gamma ray.

6. DISCUSSION

The observed gamma-ray anisotropy in the case of the Ce^{141} experiment establishes the gamma transition as being predominantly dipole, and the excited state of Pr^{141} as a $7/2^+$ level.³⁹ This is deduced from the following salient features of our results:

(i) the sign of ϵ is positive; referring to Fig. 3 this eliminates all decay schemes except

$$7/2 \rightarrow 5/2 \rightarrow 5/2 \text{ and } 7/2 \rightarrow 0,1 \rightarrow 7/2 \rightarrow 5/2;$$

(ii) during warmup the fractional change in the number of counts registered by A was about half that of B . It will be noted from Fig. 3 that if the decay scheme $7/2 \rightarrow 5/2 \rightarrow 5/2$ were correct, counting rate A would change very little during warmup, whereas with a decay scheme $7/2 \rightarrow 0,1 \rightarrow 7/2 \rightarrow 5/2$ the theoretically predicted relative changes of A and B would be close to those observed. This is illustrated in Fig. 13 where we have shown how the theoretical polar diagrams in the two cases change during warmup.

Our results do not permit us to determine whether $\Delta i_\beta=0$ or 1 because of the relatively small difference between the polar diagrams of emission of the succeeding gamma ray in the two cases. Referring to Fig. 3 we see that, even at $T=0$, the values of ϵ in the two cases are very little different (0.46 and 0.38).

³⁹ It is interesting to note that this 142-keV level of Pr^{141} has been weakly Coulomb excited with low-energy alpha particles [G. M. Temmer and N. P. Heydenburg, Phys. Rev. **93**, 351 (1954)]. Since Coulomb excitation takes place almost entirely by $E2$ transitions, this weak excitation implies a very small electric quadrupole transition matrix element as compared with most other low-lying excited states in neighboring nuclei. Although this argument cannot be made complete until the lifetime (i.e., sum of $M1$ and $E2$ matrix elements) has been determined by delayed-coincidence measurements, the facts seem to support our finding of predominant $M1$ radiation.

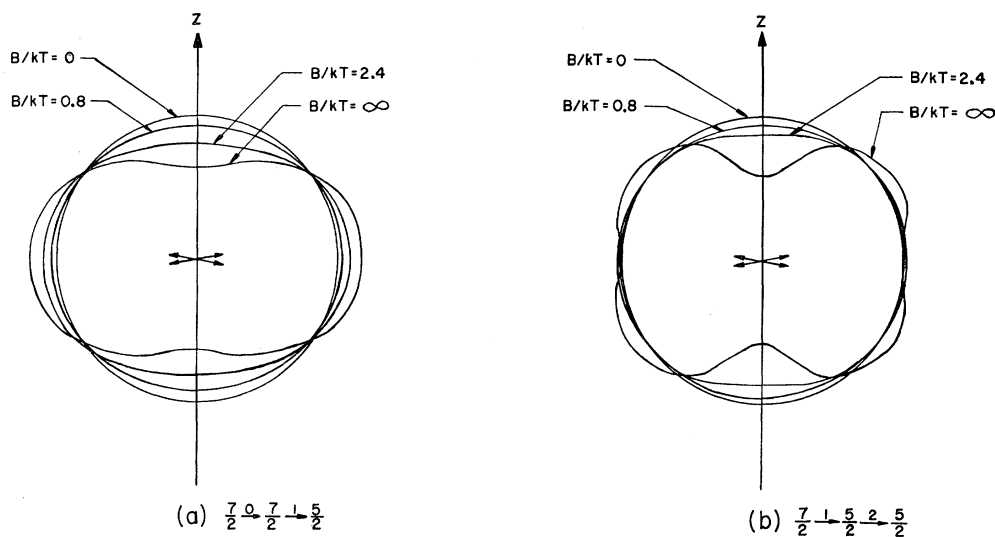


FIG. 13. Theoretical polar diagrams of gamma-ray emission for possible Ce^{141} decay schemes for several values of B/kT (B is hyperfine splitting constant; T , absolute temperature, and k , the Boltzmann constant).

From the sign of ϵ observed for the 530-keV gamma ray in the Nd^{147} experiment we can see, referring to Fig. 6, that the decay scheme $9/2 \rightarrow 7/2 \rightarrow 5/2$ can be eliminated. Since, during warmup, counting rate A increased while B decreased, and the fractional changes in the counting rates were about equal, we can eliminate the decay scheme $9/2 \rightarrow 7/2 \rightarrow 5/2$ (see Fig. 6). Thus we are left with the possibility $9/2 \rightarrow 5/2$ with Δi_β undetermined, as in the case of Ce^{141} .

Since a significant anisotropy was obtained with the 530-keV gamma ray, the existence of nuclear alignment is established, and hence the absence of an anisotropy for the 92-keV gamma ray implies that this transition is a mixture of $M1$ and $E2$ radiation.[‡] We can then deduce that the decay path including the 92-keV gamma ray must be $9/2 \rightarrow 7/2 \rightarrow 5/2$. Spin $7/2$ for the 92-keV excited state of Pm^{147} is assured since it is the only one which allows a mixture of $M1$ and $E2$ gamma radiation, and a first-forbidden beta transition.

Now the magnitude of the gamma-ray anisotropy, once the decay scheme is established, depends only upon the relative populations of the various magnetic substates, i.e., upon the temperature and the hfs constant, B . By fitting a theoretical ϵ vs $1/T$ curve to the experimental points it is thus possible to obtain a value for B . In both of our cases we do not know whether $\Delta i_\beta = 0$, or a mixture of 0 and 1; assuming it to be zero⁴⁰ we obtain for Nd^{147} , $B = 0.004 \pm 0.001 \text{ cm}^{-1}$;

[‡] Note added in proof.—After completion of this paper we discovered that the lifetime of the 92-keV transition in Pm^{147} had been accurately measured some time ago [R. L. Graham and R. E. Bell, Can. J. Phys. 31, 377 (1953)], and was found to be 2.44×10^{-9} second. This would account for the lack of anisotropy observed (see reference 45).

⁴⁰ In the extreme case of $\Delta i_\beta = 1$, the above estimates of B must be increased by about 20 percent. Actually, from the systematics of $\Delta I = 0$ beta transitions with parity change, the $\Delta i_\beta = 1$ admixture

and for Ce^{141} , assuming a pure $M1$ transition, $B = 0.0022 \pm 0.0002 \text{ cm}^{-1}$.

We may proceed to obtain estimates of the nuclear magnetic moments. For neodymium, the ratio of B for the radioactive isotope to that for a stable isotope is just the ratio of the nuclear gyromagnetic ratios [see Eq. (2)]. Using the value of $B_{145} = 0.0194 \text{ cm}^{-1}$ quoted in Sec. 3(b), taking $I_{147} = 9/2$, $I_{145} = 7/2$,⁴¹ and $\mu_{145} = 0.85$ ⁴² nuclear magnetons, we obtain $\mu_{147} = 0.22 \pm 0.05 \text{ nm}$. To obtain a value for the nuclear moment of Ce^{141} we have to make use of theory. Inserting in Eq. (2) the values³⁴ $\langle +\frac{1}{2} | N_x | -\frac{1}{2} \rangle = 1.62$, $\langle 1/r^3 \rangle_{av} = 27 \pm 7 \text{ A}^{-3}$,³³ and $I = 7/2$, we obtain $\mu_{141} = 0.16 \pm 0.06 \text{ nm}$.

The values of the magnetic moments estimated for both Nd^{147} and Ce^{141} are much smaller than those usually observed for odd-neutron nuclei. A possible explanation for this may lie in the method of deriving the theoretical values of the anisotropy. In calculating the population distribution over the various magnetic substates we have taken into account only the hyperfine splitting as obtained from the results of paramagnetic resonance, where it is normal to work with very dilute salts. In adiabatic demagnetization work, however, it is desirable to have a high concentration of magnetic ions to ensure a large heat capacity, but this causes stronger interaction magnetic fields within the crystal. The effect of these internal fields is to broaden the hyperfine energy levels of the assembly. Unfortunately there is no simple way of taking this effect into account, especially at low temperatures where a cooperative transition among the electron spins takes place. It is conceivable that they might significantly alter the population distributions

is expected to be negligible [R. W. King (private communication)].

⁴¹ B. Bleaney and H. E. D. Scovil, Proc. Phys. Soc. (London) A63, 1369 (1950).

⁴² Bleaney, Scovil, and Trenam, Phil. Mag. 43, 995 (1952).

and provide an explanation for the above discrepancies. Similar effects have been observed with Co⁶⁰ nuclei⁴³ and Mn⁵⁴ nuclei⁴⁴ in the same salt as used in our experiments, and some evidence has been obtained for the essential correctness of this explanation. We have computed the interference term due to $M1$ - $E2$ mixture in the case of Ce¹⁴¹. For reasonable values of the intensity ratio $E2/(M1+E2)$ (<15 percent) the anisotropy would not be altered significantly.

7. SUMMARY

In view of the many aspects of both solid state and nuclear physics which enter into this type of experiment, we think it worth while to emphasize here the main results:

(a) The type of nuclear alignment achieved is novel in that it is characterized by the condition that $B \gg A$, i.e., it represents "alignment" in a plane.

(b) The sign of the anisotropies, coupled with the relative change in individual counting rates between the lowest temperature reached (0.00308°K) and temperatures of essential isotropy ($\sim 0.1^\circ\text{K}$), definitely tell us the type of gamma radiation emitted; the data also permit us to eliminate most of the *a priori* possible spin and parity assignments for the initial, intermediate and final states involved in the decay chains. These conclusions are summarized in Table II. In the Nd¹⁴⁷ experiment the lack of anisotropy of the 92-keV radiation is proved to be meaningful by the simultaneous occurrence of a comparatively large anisotropy in the 530-keV radiation.

(c) Some limits can be set on the lifetimes of the gamma-ray transitions studied here. The 142-keV transition in Ce¹⁴¹ as well as the 530-keV transition in Nd¹⁴⁷ cannot have lifetimes much in excess of 10^{-10} second, simply because sizeable anisotropies were observed, and nuclear reorientation effects could not have

⁴³ E. Ambler and N. Kurti, Third International Conference on Low Temperature Physics and Chemistry (Rice Institute, Houston, 1953).

⁴⁴ J. M. Daniels and N. Kurti, Third International Conference on Low Temperature Physics and Chemistry (Rice Institute, Houston, 1953).

TABLE II. Summary of experimental results on Ce¹⁴¹ and Nd¹⁴⁷. Λ_γ : multipolarity of gamma transition.

Nucleus	E_γ (kev)	Λ_γ	Spin and parity		
			Initial	Intermediate	Final
Ce ¹⁴¹	142	$M1^a$	$7/2^-$	$7/2^+$	$5/2^+$
Nd ¹⁴⁷	92	$(M1+E2)$	$9/2^-$	$7/2^+$	$5/2^+$
Nd ¹⁴⁷	530	$E2$	$9/2^-$	$9/2^+$	$5/2^+$

^a See footnote 39.

been important.⁴⁵ The limit is in keeping with theoretical expectations for $M1$ and $E2$ transitions of these energies. On the other hand, it may be argued that the 92-keV transition in Nd¹⁴⁷, showing no anisotropy, might well have a long lifetime. However, Weisskopf's formula⁴⁶ for $M1$ radiation (which seems to be predominant from internal conversion data) of 92 keV yields a mean life $\tau_\gamma \simeq 5 \times 10^{-11}$ second, which is definitely too short to permit appreciable reorientation. §

(d) From the observed anisotropy-absolute temperature relationship, we arrive at an experimental value for the coefficient B in the spin-Hamiltonian, and hence a value for the nuclear magnetic moment. The unusually low values obtained in this manner when compared with other odd-neutron nuclei in general, and the stable isotopes of neodymium in particular, however, lead us to suspect the correctness of the assumptions made to obtain the values of B . A phenomenon produced by internal magnetic fields (not included in the spin-Hamiltonian) may well be responsible for this fact. The values of the nuclear magnetic moments are therefore in a category of much lower reliability.

8. ACKNOWLEDGMENT

We wish to thank Mr. R. Fessel for his valuable assistance with the work on Nd¹⁴⁷.

⁴⁵ N. R. Steenberg, Phys. Rev. **95**, 982 (1954).

⁴⁶ J. M. Blatt and V. F. Weisskopf, *Theoretical Nuclear Physics* (John Wiley and Sons, Inc., New York, 1952), p. 627.

§ *Note added in proof.*—However, as pointed out in the aforementioned note, the measured lifetime for this transition is 2.44×10^{-9} second, which is long enough to wipe out any intrinsic anisotropy through coupling with crystalline electric and/or magnetic fields; no conclusions can therefore be drawn concerning the $E2$ to $M1$ mixing ratio.